Title

Oxidized Cholesteryl Esters and Phospholipids in Zebrafish Larvae Fed a High Cholesterol Diet MACROPHAGE BINDING AND ACTIVATION* * This work was supported, in whole or in part, by National Institutes of Health Grants HL093767 (to Y. I. M. and L. F.),...

Journal

Journal of Biological Chemistry, 285(42)

ISSN

0021-9258

Authors

Fang, Longhou
Harkewicz, Richard
Hartvigsen, Karsten
et al.

Publication Date

2010-10-01

DOI

10.1074/jbc.m110.137257

Peer reviewed

THE JOURNAL OF BIOLOGICAL CHEMISTRY VOL. 285, NO. 42, pp. 32343–32351, October 15, 2010

Oxidized Cholesteryl Esters and Phospholipids in Zebrafish Larvae Fed a High Cholesterol Diet

*MACROPHAGE BINDING AND ACTIVATION**

Received for publication, April 22, 2010, and in revised form, August 5, 2010 Published, JBC Papers in Press, August 14, 2010, DOI 10.1074/jbc.M110.137257

Longhou Fang[‡], Richard Harkewicz[§¶], Karsten Hartvigsen[‡], Philipp Wiesner[‡], Soo-Ho Choi[‡], Felicidad Almazan[‡], Jennifer Pattison[‡], Elena Deer[‡], Tiffany Sayaphupha[‡], Edward A. Dennis[§¶], Joseph L. Witztum[‡], Sotirios Tsimikas[‡], and Yury I. Miller[‡1]

From the Departments of [‡]Medicine, [§]Pharmacology, and [¶]Chemistry and Biochemistry, University of California, San Diego, La Jolla, California 92093

A novel hypercholesterolemic zebrafish model has been developed to study early events of atherogenesis. This model utilizes optically transparent zebrafish larvae, fed a high cholesterol diet (HCD), to monitor processes of vascular inflammation in live animals. Because lipoprotein oxidation is an important factor in the development of atherosclerosis, in this study, we characterized the oxidized lipid milieu in HCD-fed zebrafish larvae. Using liquid chromatography-mass spectrometry, we show that feeding an HCD for only 2 weeks resulted in up to 70-fold increases in specific oxidized cholesteryl esters, identical to those present in human minimally oxidized LDL and in murine atherosclerotic lesions. The levels of oxidized phospholipids, such as 1-palmitoyl-2-oxovaleroyl-*sn*-glycero-3-phosphocholine, and of various lysophosphatidylcholines were also significantly elevated. Moreover, lipoproteins isolated from homogenates of HCD-fed larvae induced cell spreading as well as ERK1/2, Akt, and JNK phosphorylation in murine macrophages. Removal of apoB-containing lipoproteins from the zebrafish homogenates with an anti-human LDL antibody, as well as reducing lipid hydroperoxides with ebselen, resulted in inhibition of macrophage activation. The TLR4 deficiency in murine macrophages prevented their activation with zebrafish lipoproteins. Using biotinylated homogenates of HCD-fed larvae, we demonstrated that their components bound to murine macrophages, and this binding was effectively competed by minimally oxidized LDL but not by native LDL. These data provide evidence that molecular lipid determinants of proatherogenic macrophage phenotypes are present in large quantities in hypercholesterolemic zebrafish larvae and support the use of the HCD-fed zebrafish as a valuable model to study early events of atherogenesis.

We have recently developed a novel animal model, the cholesterol-fed zebrafish (*Danio rerio*), to study the early events of atherosclerosis (1). Zebrafish larvae are effectively studied by confocal microscopy due to their optical transparency and small size, which allows for high resolution evaluation of blood vessels in live animals. Existing transgenic lines in which fluorescent proteins are expressed under control of tissue-specific promoters make it feasible to monitor endothelial cells, leukocytes, and thrombocytes during the progress of pathological processes. Feeding zebrafish larvae a high cholesterol diet (HCD)[2] (4% cholesterol) for 10–14 days resulted in hypercholesterolemia, with associated lipid accumulation in the vascular wall, endothelial cell disorganization, increased vascular permeability, vascular recruitment of myeloid cells, and increased phospholipase A_2 activity in the vasculature, all quantitatively measured in live animals (1). In adult zebrafish, an 8–10-week HCD feeding led to hypercholesterolemia and the formation of lipid- and macrophage-rich vascular lesions. Remarkably, we observed dramatic increases in the binding of the oxidized phospholipid-specific antibody E06 to plasma apoB and apoAI lipoproteins in HCD-fed zebrafish, suggesting the considerable presence of oxidized phospholipid on LDL and HDL (1).

Lipoprotein oxidation has been suggested in many studies to significantly promote atherogenicity of LDL. In particular, specific oxidized lipid moieties mediate binding of oxidized LDL to macrophages, leading to excessive LDL uptake and the formation of lipid-loaded macrophage foam cells, a hallmark of atherosclerotic lesions (2). Oxidized phosphatidylcholines (OxPC), such as 1-palmitoyl-2-oxovaleroyl-*sn*-glycero-3-phosphocholine, mediate binding of extensively oxidized LDL (OxLDL) to scavenger receptors CD36 and SR-B1 (3–5). OxLDL binding to CD36 results in JNK-dependent OxLDL uptake and foam cell formation. Oxidative stress often leads to activation of lipoprotein-associated-phospholipase A_2 and paraoxonase, which remove the *sn2*-position acyl chain from the phosphatidylcholine (PC) molecule and produce biologically active lyso-PC (6). Lyso-PCs are involved in monocyte/macrophage recruitment and in proinflammatory gene expression in vascular cells and induce cell death (6, 7). In contrast to OxLDL, minimally oxidized LDL (mmLDL) binds to CD14 and

* This work was supported, in whole or in part, by National Institutes of Health Grants HL093767 (to Y. I. M. and L. F.), HL081862 (to Y. I. M.), GM069338 (to E. A. D., J. L. W., R. H., and Y. I. M.), and HL088093 (to J. L. W. and Y. I. M.). This work was also supported by University of California Tobacco-related Disease Program Fellowship 18FT-0137 (to L. F.) as well as a grant from the Leducq Foundation (to J. L. W. and Y. I. M.). The University of California, San Diego Cancer Center Shared Imaging Resource is funded by National Institutes of Health Specialized Support Grant P30 CA23100.

[1] To whom correspondence should be addressed. E-mail: yumiller@ucsd.edu.

[2] The abbreviations used are: HCD, high cholesterol diet; OxPC, oxidized phosphatidylcholine(s); OxLDL, extensively oxidized LDL; mmLDL, minimally oxidized LDL; OxCE, oxidized cholesteryl ester(s); MRM, multiple-reaction monitoring; CE, cholesteryl ester; PC, phosphatidylcholine; XIC, extracted ion current.

induces TLR4 (Toll-like receptor-4)-dependent macropinocytosis of lipoproteins (8, 9). This process is mediated by active components of mmLDL, oxidized cholesteryl esters (OxCE), such as those produced by oxidation of cholesteryl arachidonate with 15-lipoxygenase (9, 10). This reaction produces polyoxygenated cholesteryl ester (CE) hydroperoxides, which induce TLR4-dependent activation of ERK1/2 and JNK signaling pathways in macrophages, resulting in extensive plasma membrane ruffling and cell spreading (9). In addition, mmLDL, but not OxCE, strongly activates the PI3K/Akt signaling pathway via a TLR4-independent mechanism (9, 11).

Given the importance of these specific oxidized lipids in proinflammatory and proatherogenic mechanisms in mammals, the aim of this study was to characterize the oxidized lipid milieu in HCD-fed zebrafish larvae. We now report the finding of many OxCE and OxPC molecules in HCD-fed zebrafish larvae, identical to those reported in human mmLDL and OxLDL and in murine and human atherosclerotic lesions. Moreover, homogenates of HCD-fed larvae exhibited binding to and activation of macrophages in the manner characteristic for mmLDL and OxLDL and their biologically active lipid components. Our findings provide further evidence that molecular lipid determinants of proatherogenic macrophage phenotypes are present in large quantities in hypercholesterolemic zebrafish larvae and support the use of the HCD-fed zebrafish as a valuable model to study early processes of atherogenesis.

EXPERIMENTAL PROCEDURES

Reagents—CE standards were purchased from Sigma-Aldrich and Cayman Chemical (Ann Arbor, MI). PC, lyso-PC, and OxPC standards were purchased from Avanti Polar Lipids (Alabaster, AL). Solvents used for liquid chromatography were of chromatography grade and purchased from OmniSolv (Gibbstown, NJ). Ammonium acetate and formic acid used as liquid chromatography additives were purchased from Sigma-Aldrich. Ebselen was from Calbiochem. The E06 antibody was produced as described (12). A guinea pig anti-human apoB antibody, LDL4, generated in our laboratory, has been shown to cross-react with zebrafish apoB (1), and we also utilized a guinea pig anti-human apoAI antiserum that was shown to cross-react with zebrafish apoAI (1). Human LDL (density = 1.019–1.063 g/ml) was isolated from plasma of normolipidemic donors by sequential ultracentrifugation (13). To produce mmLDL, we incubated 50 μg/ml LDL in serum-free DMEM for 18 h with murine fibroblast cells overexpressing human 15-lipoxygenase, as reported in detail (8). To produce OxLDL, LDL (0.1 mg/ml) was incubated with 10 μM CuSO4 for 18 h at 37 °C (14). The extent of LDL oxidation was assessed by measuring thiobarbituric acid reactive substances (typically, more than 30 nmol/mg protein in OxLDL).

Fish Maintenance—Wild type (AB) zebrafish embryos were obtained by *in vitro* fertilization and natural spawning of adults maintained at 28.5 °C on a 14-h light, 10-h dark light cycle and staged as described (15). Zebrafish larvae were fed twice a day, starting at the 5th day postfertilization, with either control diet or HCD for 14 days, as described (1). All animal studies described in the paper were approved by the Animal Care and Use Committee at the University of California, San Diego.

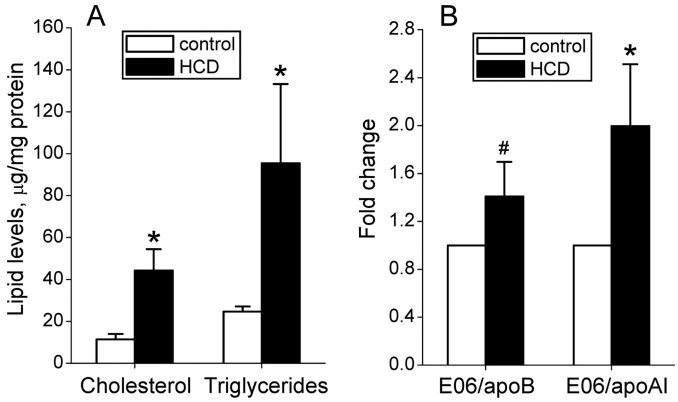

FIGURE 1. **Total cholesterol and triglyceride levels and E06 binding in homogenates of HCD-fed zebrafish larvae.** Zebrafish larvae were fed an HCD or control diet for 2 weeks, and homogenates were prepared as described under "Experimental Procedures." *A*, total cholesterol and triglyceride levels are expressed as μg of lipid/mg of protein. *B*, anti-OxPC antibody E06 binding to apoB and apoAI lipoproteins was determined using an ELISA. Shown are the mean ± S.D. (*error bars*) from three independent experiments; each measurement is from homogenates pooled from 20 larvae. *, $p < 0.05$; #, $p = 0.07$.

Cell Culture—Murine macrophage cell lines J774A.1 and RAW246.7 were maintained in DMEM supplemented with 10% heat-inactivated fetal bovine serum and 50 μg/ml Gentamicin at 37 °C in a humidified CO_2 incubator. Stable J774 cell lines expressing control or TLR4-specific shRNA were selected and used as reported previously (9). Bone marrow-derived macrophages were obtained from bone marrow cells isolated from C57BL6/J mice and differentiated with macrophage colony-stimulating factor (L929 conditioned medium) according to published protocols (16).

Zebrafish Homogenates—At the end of the feeding period, 20–50 zebrafish larvae in each experimental group were euthanized by prolonged exposure to tricaine, abdomens containing undigested food were removed, and the remaining bodies were pooled and homogenized in 200 μl of ice-cold Dulbecco's PBS or DMEM containing 10 μM butylated hydroxytoluene (an antioxidant) in an Eppendorf tube using a plastic pestle. The resultant homogenates were filtered through a 0.45-μm Dura PVDF membrane filter from Millipore (Billerica, MA). Protein content in the homogenates was determined using a Bradford assay with a kit from Pierce.

Total Cholesterol and Triglycerides—Total cholesterol and triglycerides in zebrafish larva homogenates were measured using automated enzymatic assays (Roche Applied Science and Equal Diagnostics).

Oxidized Lipoprotein Immunoassay—To analyze lipoprotein oxidation, zebrafish larva homogenate (1:200 dilution) was added to microtiter wells coated with either the guinea pig anti-human apoB or anti-human apoAI antibodies described above, which recognize zebrafish apolipoproteins (1). Oxidation-specific epitopes present on apoB or apoAI lipoproteins were then detected with biotinylated E06 monoclonal antibody using chemiluminescent techniques developed in our laboratory (12). Data are recorded as relative light units/100 ms.

Total Lipid Extraction—For total lipid extraction, 160 μl of homogenates were transferred into a glass tube, 600 μl of ice-cold methanol was added together with 17:1 (heptadecenoic

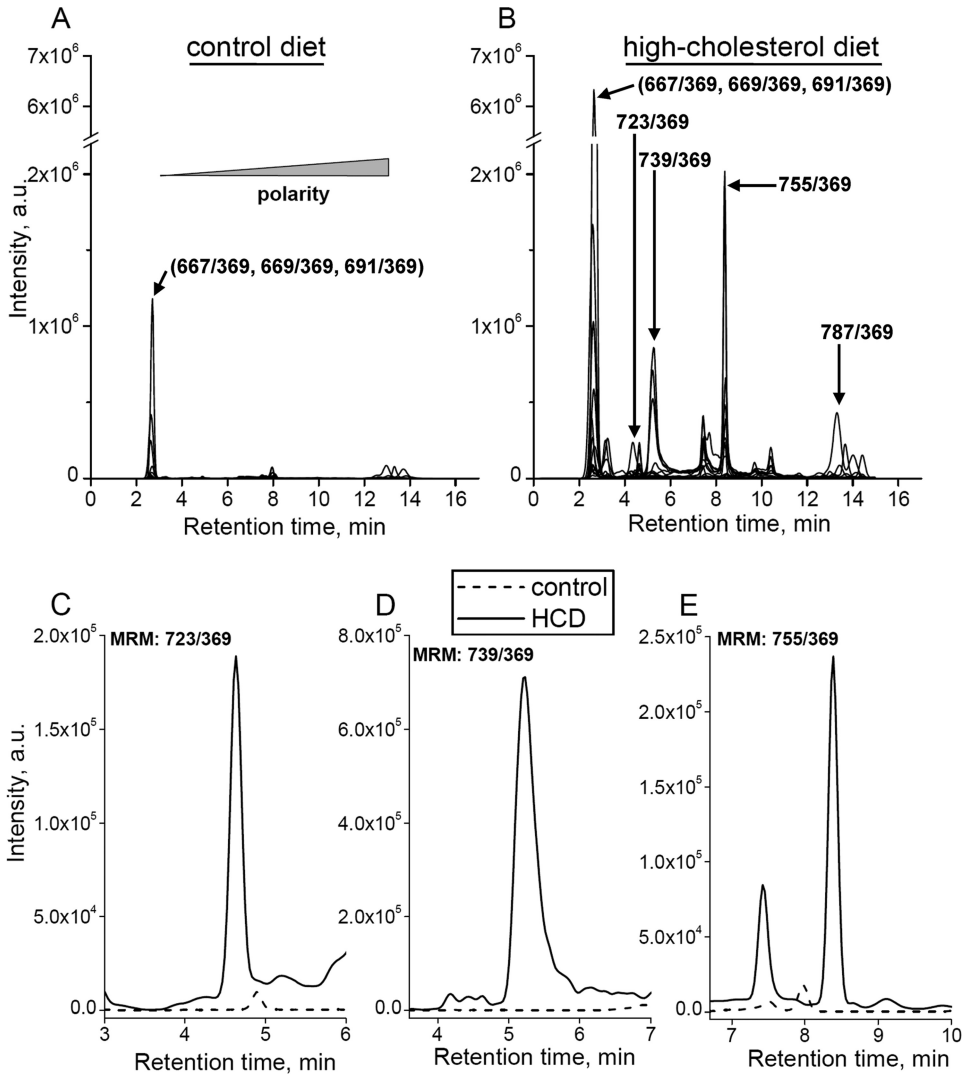

FIGURE 2. **Characterization of cholesteryl esters in HCD-fed zebrafish larvae.** Non-polar lipids were extracted from HCD-fed and control larvae and subjected to LC-MS analysis as described under "Experimental Procedures." *A* and *B*, total of 14 MRM pairs plotted for control and HCD-fed larva extracts. In normal phase HPLC, lipid molecules with increased polarity elute at later retention times due to the presence of polyoxygenated CE compounds. *C–E*, individual compounds characterized by specific retention times and MRM *m/z* values observed in control and HCD-fed larva extracts. Data in Table 1 characterize these and other CE species found in non-polar lipid extracts.

acid) CE and 17:1/17:1 PC as internal standards, and the tubes were vortexed at a maximum speed for 30 s. After centrifugation, the supernatants were transferred into fresh glass tubes. Six hundred μl of ice-cold dichloromethane and 200 μl of ice-cold DPBS were added to the supernatants and vortexed at maximum speed for 30 s. After centrifugation, the lower organic phase was transferred into a fresh glass tube using a Pasteur pipette, and the organic phase was dried under argon to ~200 μl and stored at −80 °C.

Non-polar Lipid Extraction—The organic dichloromethane phase of the total lipid extract was dried under argon gas in a 10-ml glass tube. The lipid was then reconstituted in 1.5 ml of ice-cold methanol, 60 μl water and vortexed at maximum speed for 15 s. Subsequently, 6 ml of ice-cold hexane was added to the mixture and vortexed at maximum speed for 1 min. After centrifugation, the upper hexane phase was collected into a separate glass tube, dried under argon to ~0.5 ml, and stored at −80 °C. The lower phase was used for polar lipid extraction.

Polar Lipid Extraction—The water/methanol phase from the non-polar lipid extraction procedure was supplemented with 13 μl of water and 3 ml of ice-cold dichloromethane and vortexed at a maximum speed for 1 min. After centrifugation, the lower dichloromethane phase was collected and dried under argon to ~0.5 ml and stored at −80 °C.

Liquid Chromatography—High performance liquid chromatography (HLPC) was carried out using two Shimadzu (Columbia, MD) LC-10AD high performance pumps interfaced with a Shimadzu SCL-10A controller. The sample was injected onto the liquid chromatography (LC) column using a Leap Technologies (Carrboro, NC) PAL autosampler.

Normal phase separation was employed for CE analysis using a 2.0 × 250-mm Phenomenex (Torrence, CA) silica column (Phenomenex catalogue no. 00G-4274-B0) held at 40 °C. LC buffer A was hexane/isopropyl alcohol (99.75:0.25, v/v); buffer B was hexane/isopropyl alcohol (75:25, v/v). Gradient elution was achieved using 100:0 A/B at 0 min and linearly ramped to 75:25 A/B by 30 min. A/B was ramped back to 100:0 by 32 min and held there until 50 min for column equilibration. The buffer flow rate was 0.3 ml/min. Separation optimization was achieved using both non-oxygenated and oxygenated CE standards. Non-polar lipid extracts were dried under argon and resuspended in buffer A; 25 μl of sample was injected onto the LC column for each analysis. Using an auxiliary LC pump (Scientific Systems, State College, PA), a solution of isopropyl alcohol, acetonitrile, methyl-*tert*-butyl ether, 50 mM ammonium acetate in water (45:45:5:5) at a flow rate of 0.15 ml/min was added postcolumn to the LC effluent using a high pressure mixing tee (Upchurch Scientific, Oak Harbor, WA). The CE/ammonium adduct solution thus formed was coupled to a mass spectrometer (see below) for further analysis.

Reversed phase separation was employed for PC analysis using a 2.1 × 250-mm Vydac (Hysperia, CA) C_{18} column (Vydac catalogue no. 201TP52) held at 40 °C. LC buffer A was methanol/water (75:25, v/v); buffer B was methanol; buffer A and B each contained 0.1% formic acid. Gradient elution was

achieved using 100:0 A/B at 0 min and linearly ramped to 25:75 A/B by 20 min and held there until 30 min. A/B was ramped back to 100:0 by 32 min and held there until 50 min for column equilibration. The buffer flow rate was 0.4 ml/min. Separation optimization was achieved using PC, lyso-PC, and OxPC standards. Polar lipid extracts were dried under argon and reconstituted in buffer A; 25 μl of sample was injected onto the LC column for each analysis. The PC protonated adduct solution thus formed was coupled to a mass spectrometer (see below) for further analysis.

Mass Spectrometry—All of the mass spectral analyses were performed using an Applied Biosystems (Foster City, CA) 4000 QTrap hybrid quadrupole linear ion trap mass spectrometer equipped with a Turbo V ion source.

For CE analysis, cations were formed through molecular ammonium adduction $(CE + NH_4)^+$ operating the ion source in positive electrospray mode using the following settings: CUR, 10 p.s.i.; GS1, 50 p.s.i.; GS2, 20 p.s.i.; IS, 5500 V; CAD, high; temperature, 525 °C; ihe, ON; DP, 60 V; EP, 15 V; and CXP, 10 V. The mass spectrometer was operated in multiple-reaction monitoring (MRM) mode using a collision energy setting of 25 V. MRM pairs employed in the detection method used the ammoniated CE precursor mass and the cholesterol fragment ($m/z = 369$). The cholesterol fragment is common to all CEs, regardless of their parent mass or moiety (10).

For PC, lyso-PC, and OxPC analysis, protonated adducts $(PC + H)^+$, $(lyso\text{-}PC + H)^+$, and $(OxPC + H)^+$ were formed operating the ion source in positive electrospray mode using the following settings: CUR, 10 p.s.i.; GS1, 40 p.s.i.; GS2, 0 p.s.i.; IS, 5500 V; CAD, high; temperature, 500 °C; ihe, ON; DP, 70 V; EP, 15 V; and CXP, 15 V. The mass spectrometer was operated in precursor ion scan mode using a collision energy setting of 35 V and a mass scan range of 500–900 atomic mass units. In a specified precursor ion scan mode, the mass spectrometer detects all precursor ions within the mass scan range that produce the specified fragment. In our case, PC and lyso-PC species produce the phosphocholine headgroup with $m/z = 184$, regardless of their parent mass or moiety. Applied Biosystems mass spectrometer software (Analyst 1.5.1) using the extracted ion current (XIC) option allows a search for specified precursor masses detected during the run. All masses shown throughout were rounded to the closest integer.

All samples subjected to lipid extraction had an equal protein concentration, and internal CE and PC standards were added to each sample before extraction. Thus, the data presented in the figures and in Table 1 allow for quantitative/normalized comparisons between control and HCD-fed larvae.

Macrophage Activation Assays—We have previously reported that mmLDL induced rapid and robust spreading of J774 macrophage cells (8, 9). The J774 cells were used in this assay because the quiescent cells have a round shape, which facilitates detecting spreading of activated cells. In brief, to assay macrophage spreading, J774 macrophages were incubated for 30 min with zebrafish homogenate material (see below) and then fixed with 3.7% formaldehyde and stained for F-actin with 1 μM TRITC-phalloidin (Sigma) and for nuclei with DAPI (Invitrogen). The images were captured using a DeltaVision deconvolution microscopic system operated by SoftWorx software (Applied Precision, Issaquah, WA), as described (17).

TABLE 1
Changes in the levels of non-oxygenated and oxygenated cholesteryl esters in HCD-fed zebrafish larvae

MRM[a]	Number of oxygens	Hypothetical structure of acyl chain[b]	HCD/control, change[c]
			-fold
667/369	0	Linoleate	4–9
669/369	0	Oleate	11–13
691/369	0	Arachidonate	5–9
681/369	1	OxoODE	10–36
683/369	1	HODE	35–40
699/369	2	HpODE	10–12
705/369	1	OxoETE	15–40
707/369	1	HETE	25–30
723/369	2	HpETE	40–50
739/369	3	Epoxy-HpETrE	50–70
755/369	4	Bicyclic endoperoxide	10–25
787/369	6	Serial cyclic peroxide	15–25

[a] The first member of the MRM pair is the *m/z* of the precursor ammonium adduct CE cation $(CE + NH^4)^+$, and the second member is the *m/z* of their corresponding fragment ion; in these MRMs, the second member is always the cholesterol cation ($m/z = 369$).
[b] Oxygenated acyl chains may have positional and/or stereo chemistry different from the examples given here: linoleate, (9*Z*,12*Z*)-octadecadienoate; oleate, (9*Z*)-octadecenoate; arachidonate, (5*Z*,8*Z*,11*Z*,14*Z*)-eicosatetraenoate; OxoODE, 13-oxo-(9*Z*,11*E*)-octadecadienoate; HODE, (13*S*)-hydroxy-(9*Z*,11*E*)-octadecadienoate; HpODE, (13*S*)-hydroperoxy-(9*Z*,11*E*)-octadecadienoate; OxoETE, 15-oxo-(5*Z*,8*Z*,11*Z*,13*E*)-eicosatetraenoate; HETE, (15*S*)-hydroxy-(5*Z*,8*Z*,11*Z*,13*E*)-eicosatetraenoate; HpETE, (15*S*)-hydroperoxy-(5*Z*,8*Z*,11*Z*,13*E*)-eicosatetraenoate; epoxy-HpETrE, (11,12)-epoxy-(15*S*)-hydroperoxy-(5*Z*,8*Z*,13*E*)-eicosatrienoate; bicyclic endoperoxide, (9,11)-epidioxy-(15*S*)-hydroperoxy-(5*Z*,13*E*)-prostadienoate; serial cyclic peroxide, (5*S*)-hydroperoxy-(6,8),(9,11)-diepidioxy-(12*E*,14*Z*)-eicosadienoate.
[c] Ranges of values from three independent experiments.

Murine RAW macrophages were used in our previous studies to assay phosphorylation of signaling molecules in cells activated with mmLDL (18). Thus, we incubated RAW cells for 20 min with native or fractionated (see below) zebrafish larva homogenates. The cell lysates were subjected to SDS-PAGE, transferred to a PVDF membrane, and probed with the antibodies against phospho-Akt (Ser^{473}), phospho-ERK1/2 (Thr^{202}/Tyr^{204}), phospho-SAPK/JNK (Thr^{183}/Tyr^{185}), total ERK1/2, total Akt, or GAPDH (Cell Signaling Technology, Danvers, MA). In addition, cell signaling experiments were performed with control and TLR4 knockdown stable J774 macrophage cell lines established in our earlier work (9).

Fractionation of Zebrafish Homogenates for Cell Activation Experiments—To isolate lipoproteins, zebrafish homogenates were supplemented with NaBr to adjust density to 1.21 and subjected to ultracentrifugation for 40 h at 32,000 rpm in a Beckman 50.3 Ti rotor. The top (lipoprotein fraction) and bottom (lipoprotein-deficient fraction) layers were collected and dialyzed against PBS and then against DMEM to use them directly in macrophage activation assays. To confirm the presence of lipoproteins, each fraction was analyzed in native agarose gel electrophoresis with Fat Red staining (Helena Laboratories).

Some zebrafish larva homogenates were subjected to immunodepletion with the LDL4 antibody (guinea pig anti-human apoB). In brief, 200 μg of homogenates were incubated overnight at 4 °C with 2 μg of nonspecific IgG or LDL4, followed by incubation with Protein G-agarose beads. Bead-immobilized immune complexes were separated by centrifugation and subjected to SDS-PAGE and immunoblotting with LDL4 to detect

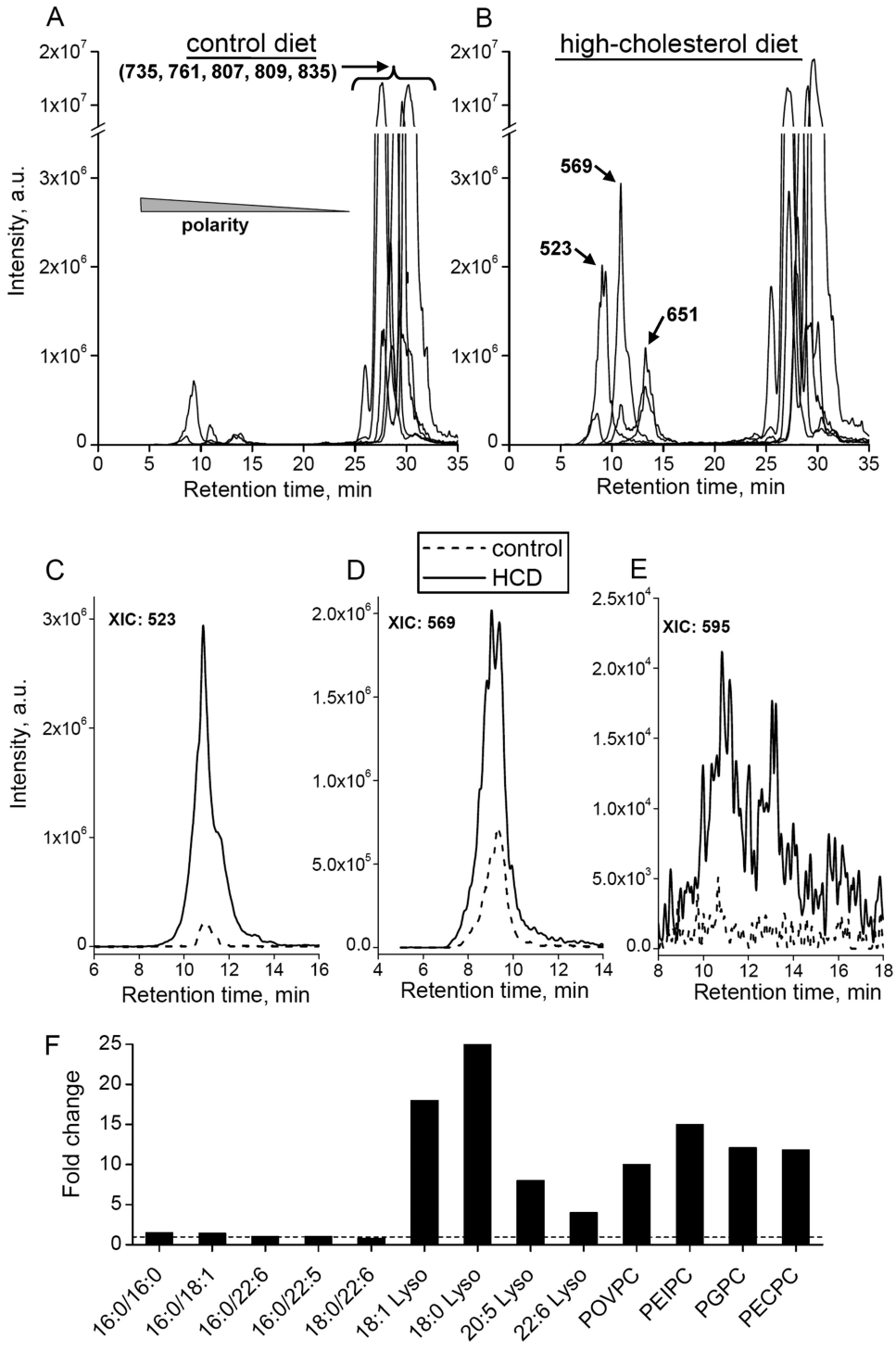

FIGURE 3. **Characterization of phosphatidylcholines in HCD-fed zebrafish larvae.** Polar lipids extracted from HCD-fed and control larvae were subjected to LC-MS analysis as described under "Experimental Procedures." *A* and *B*, a total of 11 XICs, which allows for search of specified precursor masses (m/z = 184 for PC), are plotted for control and HCD-fed larva extracts. In reverse phase HPLC, more polar lipid molecules elute at earlier retention times and consist of oxygenated or lyspo-PC compounds. *C–E*, individual compounds characterized by specific retention times and XIC m/z values observed in control and HCD-fed larva extracts: XIC 523, 18:1 lyso-PC; XIC 569, 22:6 lyso-PC; XIC 595, POVPC. *F*, -fold change of the levels of specific PC in HCD-fed larva polar extracts over the control. Data were normalized to internal standards in each sample. *POVPC*, 1-palmitoyl-2-(5′-oxo-valeroyl)-*sn*-glycero-3-phosphocholine; *PEIPC*, 1-palmitoyl-2-(5,6-epoxyisoprostane E2)-*sn*-glycero-3-phosphocholine; *PECPC*, 1-palmitoyl-2-(5,6-epoxycyclopentane)-*sn*-glycero-3-phosphocholine; *PGPC*, 1-palmitoyl-2-glutaryl-*sn*-glycero-3-phosphocholine.

apoB. Immunodepleted samples were used in macrophage activation experiments.

Macrophage Binding Assay—Binding of biotinylated zebrafish homogenates to J774 murine macrophages plated in microtiter wells was assessed by a chemiluminescent binding assay as described by Binder *et al.* (19) with modifications. In short, the >100-kDa fraction of zebrafish homogenate was isolated using a centrifugal filter concentrator (Millipore, Billerica, MA) and biotinylated according to manufacturer's protocol (catalog no. 21326; Pierce). The biotinylated homogenates of equal protein concentration were serially diluted and tested for binding to adherent macrophages. Because we observed stronger binding of homogenates of HCD-fed zebrafish compared with the control homogenates, fixed concentrations of the biotinylated control and HCD-fed zebrafish homogenates (6.5 and 2.5 μg/ml, respectively) were selected to obtain approximately equal binding (B_0) for competition experiments. The zebrafish homogenates at fixed concentrations were incubated with serially diluted competitors and controls in 1% bovine serum albumin in PBS (1% BSA-PBS) at concentrations/dilutions indicated in the figures. The ligand-competitor solutions were incubated overnight at 4 °C.

J774 murine macrophages were cultured in 10% fetal bovine serum in DMEM (DMEM-10) and plated in 100 μl of L929-conditioned medium at 25,000 cells/well in sterile 96-well flat-bottom white plates (Greiner Bio-One). The plating medium consisted of 20% L929-conditioned DMEM-10 and 80% fresh DMEM-10 and served as a source of growth factors, including M-CSF. After 72 h, plates were washed gently 5 times with PBS using a microtiter plate washer (Dynex Technologies, Chantilly, VA), and wells were blocked with 200 μl of ice-cold 1% BSA-PBS for 30 min, whereas plates were kept on ice. After washing, macrophages

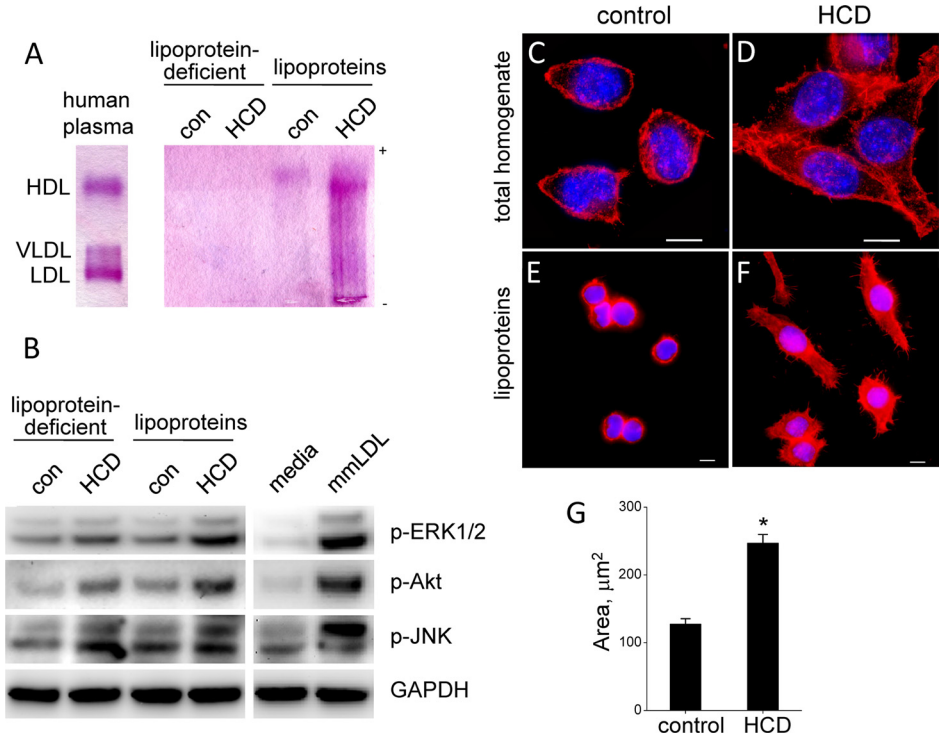

FIGURE 4. **Lipoproteins in zebrafish homogenates activate murine macrophages.** *A*, lipoprotein and lipoprotein-deficient fractions isolated from zebrafish larva homogenates by ultracentrifugation were analyzed in native agarose gel electrophoresis with Fat Red staining. A human plasma sample was used as a positive control. *B*, RAW macrophages were incubated for 20 min with lipoprotein and lipoprotein-deficient fractions isolated from control and HCD-fed zebrafish larvae, and cell lysates were analyzed by immunoblot. RAW cells activated with mmLDL were used as a positive control. *C–F*, J774 macrophages were incubated for 20 min with 1 μg/μl (protein) of homogenates of control or HCD-fed zebrafish larvae (*C* and *D*) or with lipoproteins isolated from zebrafish homogenates by ultracentrifugation (*E* and *F*). At the end of incubation, cells were fixed and stained to visualize F-actin cytoskeleton (*red*) and nuclei (*blue*). *Scale bar*, 10 μm. *G*, cell surface area were measured in cells incubated with lipoprotein fractions isolated from control and HCD-fed zebrafish homogenates. Shown are the mean ± S.E. ($n = 50$); *, $p < 0.001$. *p-*, phospho-.

were incubated with ice-cold ligand and ligand-competitor solutions (100 μl/well) for 2 h on ice, washed again, and fixed with ice-cold 3.7% formaldehyde in PBS for 30 min in the dark. After fixing the macrophages, the remainder of the assay was carried out at room temperature. Macrophage-bound biotinylated zebrafish homogenate was detected with NeutrAvidin-conjugated alkaline phosphatase (Pierce), LumiPhos 530 (Lumigen, Southfield, MI), and a Dynex luminometer (Dynex Technologies). Data were recorded as relative light units counted per 100 ms and expressed as a ratio of binding in the presence of competitor (B) divided by binding in the absence of competitor (B_0).

RESULTS

Characterization of Oxidized Lipids in HCD-fed Zebrafish Larvae— We have previously demonstrated that in HCD-fed adult zebrafish, plasma levels of total cholesterol were 4-fold higher than in control plasma. In addition, the E06 antibody to OxPC bound strongly to zebrafish plasma lipoproteins (3). However, adult zebrafish are not optically transparent and thus not suitable for confocal imaging. The goal of this study was to characterize lipids in HCD-fed zebrafish larvae, which are an emerging model for *in vivo* confocal monitoring of vascular processes. Because drawing blood from 15–20-day postfertilization larvae is impractical, if not impossible, all experiments in this study were performed with homogenates of larvae from which abdomens have been removed to exclude undigested food from the analysis.

Feeding HCD to zebrafish larvae resulted in 4-fold increases in both total cholesterol and triglycerides over the levels observed in controls (Fig. 1*A*), demonstrating that HCD causes hypercholesterolemia in larvae as it did in adult fish (1). The levels of OxPC, as measured by E06 binding, were increased significantly in apoAI lipoproteins ($p < 0.05$) and nearly significantly in apoB lipoproteins ($p = 0.07$) (Fig. 1*B*).

Using HPLC-MS, we characterized CE and PL in non-polar and polar lipid extracts from control and HCD-fed larvae. Non-oxygenated CEs (cholesteryl arachidonate, linoleate, and oleate) were increased 4–13-fold in HCD-fed larvae (Fig. 2, *A* and *B*, and Table 1), indicating increases in circulating lipoproteins and/or deposits of tissue lipid droplets. Remarkably, oxygenated CEs increased as much as 10–70-fold (Fig. 2, *C–E*, and Table 1), suggesting that the HCD feeding induced strong lipoprotein oxidation. Using similar techniques, we have previously demonstrated the presence of oxygenated CEs with m/z of 723, 739, 755, and 787 (ammonium adducts) in mmLDL and in mouse atherosclerotic lesions (10).

We also quantified non-modified PC and selected oxidized PC lipids (1-palmitoyl-2-oxovaleroyl-*sn*-glycero-3-phosphocholine (*POVPC*), 1-palmitoyl-2-(5,6-epoxyisoprostane E2)-*sn*-glycero-3-phosphocholine (*PEIPC*), 1-palmitoyl-2-glutaryl-*sn*-glycero-3-phosphocholine (*PGPC*), and 1-palmitoyl-2-(5,6-epoxycyclopentane)-*sn*-glycero-3-phosphocholine (*PECPC*)) and lyso-PC (Fig. 3). In response to the HCD, there was a rather robust generation of all four monitored OxPC as well as lyso-PC, with increases varying from 5- to 25-fold (Fig. 3*F*). Absolute levels of lyso-PC were significantly higher than the levels of OxPC species in these samples, suggesting the presence of considerable phospholipase A_2 activity. Both lyso-PC and OxPC have been demonstrated to exert proinflammatory and proatherogenic properties (5, 6, 20, 21). Because the lipid values were normalized to the protein concentration in samples, no significant changes were observed in the non-oxidized PC levels, reflecting physiological PL content in cellular membranes.

Lipoproteins in Homogenates of HCD-fed Zebrafish Larvae Activate MAPK and Akt Signaling Pathways and Induce Macrophage Spreading—The OxCE and OxPC identified in HCD-fed larva homogenates (Figs. 2 and 3) have been demonstrated to be part of oxidized mammalian lipoproteins and to

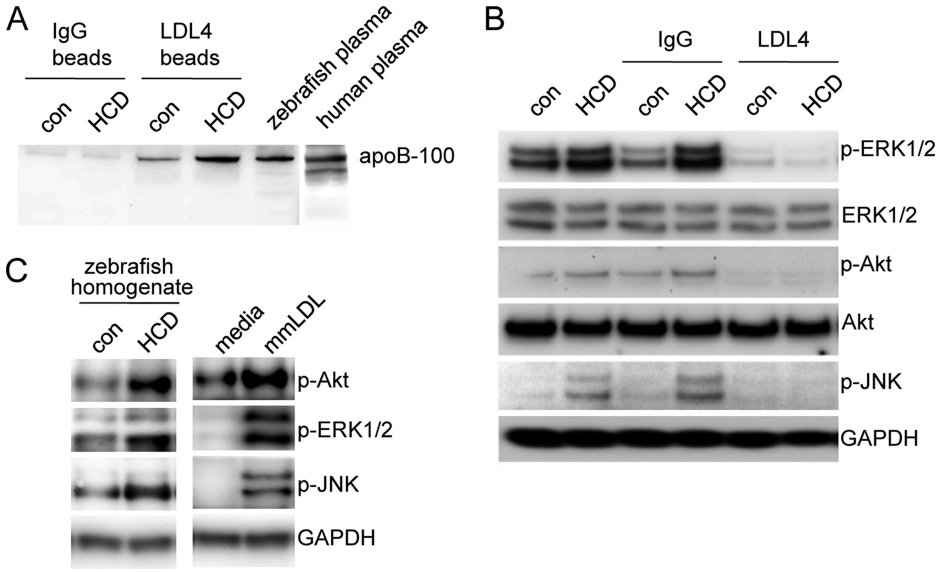

FIGURE 5. **Homogenates of HCD-fed zebrafish larvae contain apoB lipoproteins and activate primary macrophages.** *A*, homogenates of control and HCD-fed larvae were incubated with LDL4 (antibody to human LDL) or control IgG, followed by incubation with Protein G beads. The beads were separated by centrifugation (supernatants were used in *B*) and run on SDS-PAGE, followed by Western blot with LDL4. Plasma isolated from adult zebrafish (1:10) and human plasma (1:50) were used as a positive control (all samples were run on the same gel, but the stronger signal from human plasma was detected at a shorter exposure time). *B*, RAW macrophages were incubated for 20 min with 1 μg/μl (protein) homogenates of control or HCD-fed zebrafish larvae or with the homogenates depleted from apoB lipoproteins (supernatants from *A*). Cell lysates were subjected to SDS-PAGE and immunoblotting with the indicated antibodies. *C*, bone marrow-derived macrophages were incubated for 20 min with 1 μg/μl (protein) homogenates of control or HCD-fed zebrafish larvae, and cell lysates were subjected to SDS-PAGE and immunoblot. Cells activated with mmLDL were used as a positive control. *p*-, phospho-.

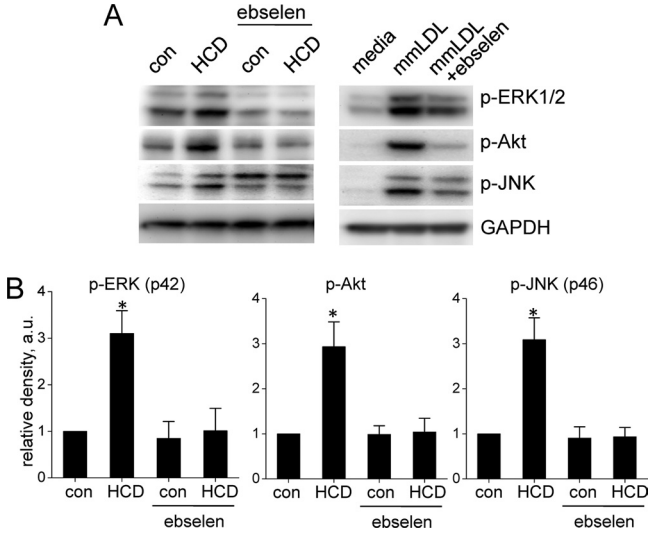

FIGURE 6. **Ebselen inhibits macrophage activation with zebrafish larva lipoproteins.** *A*, lipoprotein fractions of zebrafish larva homogenates were pretreated for 1 h with 50 μM ebselen (hydroperoxide reducing agent) and then incubated with RAW macrophages for 20 min. Cell lysates were subjected to SDS-PAGE and immunoblot. Cells activated with mmLDL were used as a positive control. *B*, immunoblot bands from three experiments were quantified. Shown are the mean ± S.E.; *, $p < 0.05$. *p*-, phospho-.

activate mammalian macrophages (5, 22). Thus, we tested if the zebrafish larva homogenates contained lipoproteins. The homogenates of control and HCD-fed larvae were subjected to ultracentrifugation to separate fractions with d<1.21 (lipoprotein fraction) and d>1.21 (lipoprotein-deficient fraction). The presence of lipoproteins in the $d < 1.21$ fraction and their absence in the $d > 1.21$ fraction were confirmed in agarose gel electrophoresis with neutral lipid staining (Fig. 4*A*). As with plasma isolated from adult fish (1), HCD feeding induced dramatic increases in lipoprotein levels in zebrafish larva homogenates.

Lipoproteins isolated from HCD-fed larvae induced phosphorylation of ERK1/2, Akt, and JNK in mouse macrophages (Fig. 4*B*). Activation of these kinases has been reported in our previous work in macrophages stimulated with mmLDL and OxCE (9, 10, 18, 23). HCD feeding also resulted in the accumulation of non-lipoprotein active components, as is evident from the blot in Fig. 4*B*.

Both total larva homogenates and the lipoprotein fraction of HCD-fed zebrafish induced rapid and robust macrophage spreading (Fig. 4, *C* and *G*), the effect also characteristic of mmLDL- and OxLDL-induced activation of macrophages (8).

Next, we tested if zebrafish larva homogenates contain apoB. Homogenates were incubated with LDL4, a polyclonal antibody raised against human LDL, which reacts with both human and zebrafish apoB (1), and the immune complexes were immobilized on Protein G beads. The presence of apoB-100 on the LDL4 beads was demonstrated in Western blot (Fig. 5*A*). The homogenates in which apoB was absorbed by LDL4 beads did not activate macrophages (Fig. 5*B*), strongly suggesting that the oxidized moieties responsible for the biological activity were present on apoB lipoproteins and, possibly, on apoB that may have adsorbed to some lipid-containing cellular components during homogenization. This may explain the findings in Fig. 4*B* that some macrophage-activating components were present in the lipoprotein-deficient fraction.

The results with macrophage cell lines J774 and RAW (Figs. 4 and 5, *A* and *B*) were validated in experiments with primary cells. Bone marrow-derived macrophages incubated with homogenates of HCD-fed larvae showed increased levels of phosphorylated Akt, ERK1/2, and JNK as well (Fig. 5*C*).

Ebselen and TLR4 Deficiency Inhibit Macrophage Activation with Lipoproteins from HCD-fed Zebrafish Larvae—We previously demonstrated that OxCE are responsible for many of the biological effects of mmLDL in activating macrophages (10). We further demonstrated that the synthetic agent ebselen, which has the capacity to selectively reduce hydroperoxides on oxidized lipids, was able to inhibit the ability of such OxCE and mmLDL to activate macrophages (10). Here, we found that pretreatment of the larva lipoproteins with ebselen also inhibited phosphorylation of ERK1/2, Akt, and JNK1 (p46) in macrophages (Fig. 6), indicating the presence of hydroperoxides that were responsible for the biological activities measured. Interestingly, in contrast to mmLDL, lipoproteins from control

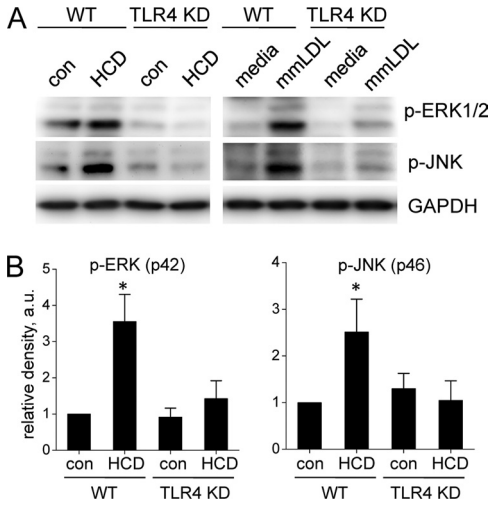

FIGURE 7. **TLR4 deficiency inhibits macrophage activation with zebrafish larva lipoproteins.** *A*, J774 macrophages stably expressing control or TLR4 shRNA (WT and TLR4 *KD*, respectively) were incubated for 20 min with the lipoprotein fraction of control and HCD-fed zebrafish larva homogenates. Cell lysates were subjected to SDS-PAGE and immunoblot. Cells activated with mmLDL were used as a positive control. *B*, immunoblot bands from three experiments were quantified. Shown are the mean ± S.E.; *, $p < 0.05$; *p-*, phospho-.

and HCD-fed zebrafish, treated with ebselen, induced activation of JNK2 (p54); the mechanism of this effect is unknown.

Because many biological effects of mmLDL and OxCE are mediated by the macrophage receptor TLR4 (8, 9, 24), next we tested whether the TLR4 deficiency would inhibit macrophage activation with zebrafish lipoproteins. Indeed, TLR4 knockdown in J774 macrophages resulted in significant reductions in phosphorylation of ERK1/2 and JNK (Fig. 7), two kinases demonstrated to be activated in a TLR4-dependent manner in macrophages stimulated with mmLDL (9, 23).

Homogenates of HCD-fed Zebrafish Larvae Share Ligand Recognition Determinants with mmLDL—Because many of the OxPC and OxCE species identified in Figs. 2 and 3 have been documented to determine OxLDL and mmLDL binding to macrophages, we tested whether homogenates of zebrafish larvae bound to macrophages. In these experiments, requiring relatively large quantities of zebrafish material, we separated the homogenates using size exclusion centrifugal filters and found that only a >100-kDa fraction bound to macrophages (not shown). Thus, the >100-kDa fractions were used in experiments presented in Fig. 8. At every concentration added, there was higher binding with the HCD-fed larva homogenates compared with the control homogenates (Fig. 8*A*). In competition experiments, the addition of mmLDL inhibited up to 45% of macrophage recognition of the HCD homogenate but had no effect on binding of the control homogenate (Fig. 8*C*). OxLDL showed minimal competition, whereas native LDL did not affect binding of either homogenate to the macrophages (Fig. 8, *B* and *D*). These results agree with the data shown in Figs. 2 and 3 in which we observed the greatest enrichment in polyoxygenated CE hydroperoxides and relatively modest increases in OxPC in HCD-fed larvae.

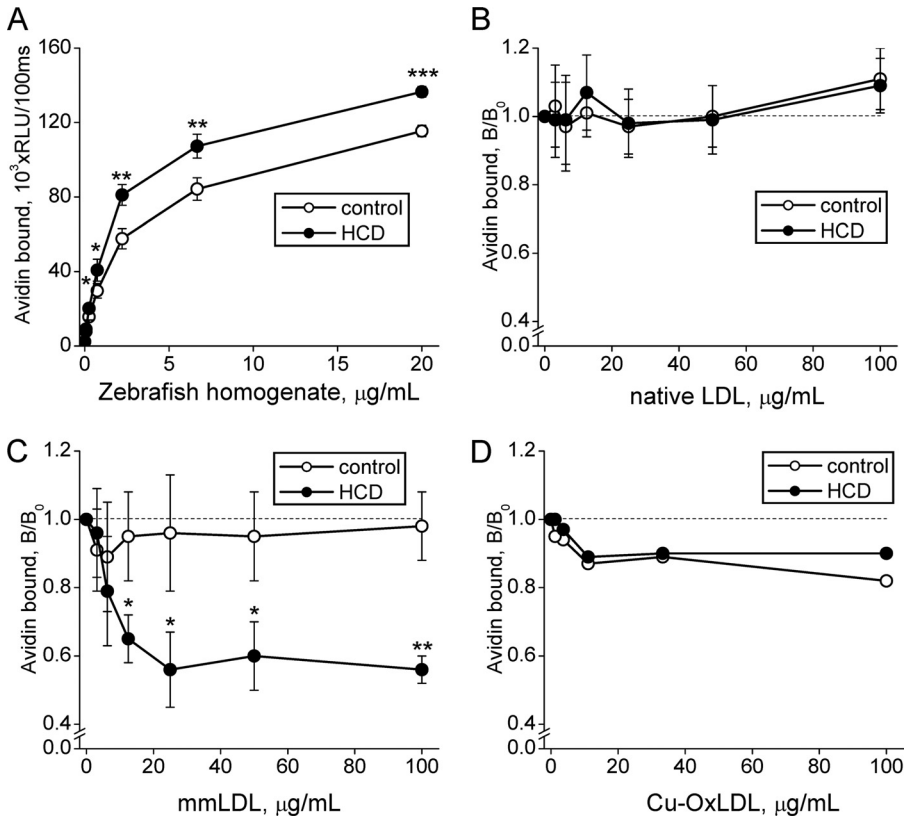

FIGURE 8. **Binding of homogenates of HCD-fed zebrafish to macrophages.** The >100-kDa fractions of homogenates of control and HCD-fed zebrafish were biotinylated and tested for specific binding to J774 macrophages. *A*, dose dependence of biotinylated homogenates binding to macrophages. *B–D*, in competition experiments, the concentrations of biotinylated control and HCD homogenates were adjusted to yield identical initial binding (B_0), 6.5 and 2.5 μg/ml, respectively. The homogenates were preincubated with competitors, native LDL, mmLDL, or OxLDL, added at the concentrations indicated on the graphs, and then tested for macrophage binding as described under "Experimental Procedures." Each data point represents the mean of triplicate wells in a plate, and the *error bar* represents the S.D. of four independent plates (mean ± S.D.). *, $p < 0.05$; **, $p < 0.01$; ***, $p < 0.001$.

Collectively, these data suggest that HCD feeding leads to accumulation in zebrafish larvae of biologically active oxidized lipoproteins similar to current mmLDL and OxLDL models used in studies of the pathophysiology of mammalian atherosclerosis.

DISCUSSION

Accumulating evidence suggests that oxidized lipoproteins play an important role in atherogenesis in humans and in animal models (2, 5, 25). Our novel zebrafish model of early processes of atherosclerosis offers a particularly attractive experimental model because of the marked extent to which plasma lipoproteins appear to be oxidized

in HCD-fed zebrafish, as demonstrated in our previous work (1) and significantly amplified in the current study. In the current work, we wished to specifically study the oxidized lipid milieu in HCD-fed zebrafish larvae because these small (5-mm-long) young animals are optically transparent during the larval stage and suitable for *in vivo* imaging studies using confocal microscopy. Indeed, we demonstrated that HCD feeding, for as little as 2 weeks, resulted in remarkable accumulation of oxidized CE and PC species (Figs. 1–3), many of which have been shown to possess important proinflammatory and proatherogenic properties. We tested several of these atherogenic effects and found that HCD-fed zebrafish homogenates and lipoproteins isolated from the homogenates activated murine macrophages in a manner consistent with mmLDL and OxLDL activation (*i.e.* cell spreading and phosphorylation of ERK1/2, JNK, and Akt) (Fig. 4). Importantly, these effects were inhibited by removal of apoB lipoproteins as well as by reduction of lipid hydroperoxides, whose presence is critical for mmLDL activity (Figs. 5 and 6). Macrophage expression of TLR4, which mediates many mmLDL and OxCE effects, was also important for macrophage activation with zebrafish lipoproteins (Fig. 7). In addition, HCD-fed zebrafish homogenates bound to murine macrophages, and this binding was effectively competed by mmLDL (Fig. 8).

These studies demonstrated that a 2-week HCD feeding of zebrafish larvae resulted in the development of many characteristics of the initial stages of lesion formation in zebrafish: (i) a profile of oxidized lipids characterized by a significant enrichment with early products of CE oxidation (Fig. 2 and Table 1), (ii) mmLDL-like profile of macrophage activation and its dependence on the presence of hydroperoxides (Figs. 4–7), and (iii) the presence of mmLDL-like determinants responsible for specific macrophage binding (Fig. 8). The finding of apoB lipoproteins that had an mmLDL-like "phenotype" with regard to the presence of OxCE and the ability to induce biological changes in macrophages is consistent with our earlier results demonstrating that lipid uptake by macrophages in zebrafish vascular lesions was dependent on the expression of functional TLR4, the macrophage receptor responsible for mmLDL-mediated lipid uptake in cell culture experiments (1, 9). Undoubtedly, there are also more extensively oxidized LDL lipoproteins and probably even oxidized HDL lipoproteins as well (Fig. 1). Further work will be needed to fully characterize these oxidized lipoproteins. However, these data suggest that cholesterol-fed zebrafish will be a useful model in which to study the efficacy of various antioxidant compounds.

Another important conclusion from this study is that HCD feeding of even a phylogenetically lower species, fish, results in profound lipid oxidation producing exactly the same OxCE, lyso-PC, and OxPC species as found in human oxidized LDL and in human and mouse atherosclerotic lesions. The presentation of these oxidized lipids in zebrafish larvae is probably the same as in mammalian lipoproteins because the zebrafish homogenates activated mouse macrophages in the same manner as does human mmLDL. These results support the validity of our experiments in which we transferred mouse macrophages into zebrafish vascular lesions and monitored accumulation of endogenous zebrafish lipids in these mouse macrophages (1). We believe that these experiments closely replicate the processes occurring in mouse atherosclerotic lesions. The advantage of conducting these studies in zebrafish larvae is that macrophage lipid accumulation can be monitored temporally in live animals.

Taken together, the results of this study suggest that HCD feeding initiates in zebrafish larvae profound lipid oxidation and that resulting oxidized lipid species closely match those found in mammalian atherosclerosis and activate important proatherogenic mechanisms. These data are important for accurate interpretation of future experiments using the novel zebrafish model of early processes of atherosclerosis.

REFERENCES

1. Stoletov, K., Fang, L., Choi, S. H., Hartvigsen, K., Hansen, L. F., Hall, C., Pattison, J., Juliano, J., Miller, E. R., Almazan, F., Crosier, P., Witztum, J. L., Klemke, R. L., and Miller, Y. I. (2009) *Circ. Res.* **104,** 952–960
2. Glass, C. K., and Witztum, J. L. (2001) *Cell* **104,** 503–516
3. Boullier, A., Friedman, P., Harkewicz, R., Hartvigsen, K., Green, S. R., Almazan, F., Dennis, E. A., Steinberg, D., Witztum, J. L., and Quehenberger, O. (2005) *J. Lipid Res.* **46,** 969–976
4. Podrez, E. A., Poliakov, E., Shen, Z., Zhang, R., Deng, Y., Sun, M., Finton, P. J., Shan, L., Gugiu, B., Fox, P. L., Hoff, H. F., Salomon, R. G., and Hazen, S. L. (2002) *J. Biol. Chem.* **277,** 38503–38516
5. Berliner, J. A., and Watson, A. D. (2005) *N. Engl. J. Med.* **353,** 9–11
6. Oörni, K., and Kovanen, P. T. (2009) *Curr. Opin. Lipidol.* **20,** 421–427
7. Takabe, W., Kanai, Y., Chairoungdua, A., Shibata, N., Toi, S., Kobayashi, M., Kodama, T., and Noguchi, N. (2004) *Arterioscler. Thromb. Vasc. Biol.* **24,** 1640–1645
8. Miller, Y. I., Viriyakosol, S., Binder, C. J., Feramisco, J. R., Kirkland, T. N., and Witztum, J. L. (2003) *J. Biol. Chem.* **278,** 1561–1568
9. Choi, S. H., Harkewicz, R., Lee, J. H., Boullier, A., Almazan, F., Li, A. C., Witztum, J. L., Bae, Y. S., and Miller, Y. I. (2009) *Circ. Res.* **104,** 1355–1363
10. Harkewicz, R., Hartvigsen, K., Almazan, F., Dennis, E. A., Witztum, J. L., and Miller, Y. I. (2008) *J. Biol. Chem.* **283,** 10241–10251
11. Miller, Y. I., Worrall, D. S., Funk, C. D., Feramisco, J. R., and Witztum, J. L. (2003) *Mol. Biol. Cell* **14,** 4196–4206
12. Palinski, W., Hörkkö, S., Miller, E., Steinbrecher, U. P., Powell, H. C., Curtiss, L. K., and Witztum, J. L. (1996) *J. Clin. Invest.* **98,** 800–814
13. Havel, R. J., Eder, H. A., and Bragdon, J. H. (1955) *J. Clin. Invest.* **34,** 1345–1353
14. Boullier, A., Li, Y., Quehenberger, O., Palinski, W., Tabas, I., Witztum, J. L., and Miller, Y. I. (2006) *Arterioscler. Thromb. Vasc. Biol.* **26,** 1169–1176
15. Kimmel, C. B., Ballard, W. W., Kimmel, S. R., Ullmann, B., and Schilling, T. F. (1995) *Dev. Dyn.* **203,** 253–310
16. Sawka-Verhelle, D., Escoubet-Lozach, L., Fong, A. L., Hester, K. D., Herzig, S., Lebrun, P., and Glass, C. K. (2004) *J. Biol. Chem.* **279,** 17772–17784
17. Miller, Y. I., Chang, M. K., Funk, C. D., Feramisco, J. R., and Witztum, J. L. (2001) *J. Biol. Chem.* **276,** 19431–19439
18. Wiesner, P., Choi, S. H., Almazan, F., Benner, C., Huang, W., Diehl, C. J., Gonen, A., Butler, S., Witztum, J. L., Glass, C. K., and Miller, Y. I. (2010) *Circ. Res.* **107,** 56–65
19. Binder, C. J., Hörkkö, S., Dewan, A., Chang, M. K., Kieu, E. P., Goodyear, C. S., Shaw, P. X., Palinski, W., Witztum, J. L., and Silverman, G. J. (2003) *Nat. Med.* **9,** 736–743
20. Hartvigsen, K., Chou, M. Y., Hansen, L. F., Shaw, P. X., Tsimikas, S., Binder, C. J., and Witztum, J. L. (2009) *J. Lipid Res.* **50,** S388–S393
21. Hazen, S. L. (2008) *J. Biol. Chem.* **283,** 15527–15531
22. Miller, Y. I., Choi, S. H., Fang, L., and Tsimikas, S. (2010) *Subcell. Biochem.* **51,** 229–251
23. Miller, Y. I., Viriyakosol, S., Worrall, D. S., Boullier, A., Butler, S., and Witztum, J. L. (2005) *Arterioscler. Thromb. Vasc. Biol.* **25,** 1213–1219
24. Bae, Y. S., Lee, J. H., Choi, S. H., Kim, S., Almazan, F., Witztum, J. L., and Miller, Y. I. (2009) *Circ. Res.* **104,** 210–218
25. Tsimikas, S., Brilakis, E. S., Miller, E. R., McConnell, J. P., Lennon, R. J., Kornman, K. S., Witztum, J. L., and Berger, P. B. (2005) *N. Engl. J. Med.* **353,** 46–57